REGULAR PAPER

Excitation energy pathways in the photosynthetic units of reaction center LM- and H-subunit deletion mutants of *Rhodospirillum rubrum*

**Sergiu Amarie · Domenico Lupo · Martin O. Lenz ·
Rudolf Saegesser · Robin Ghosh · Josef Wachtveitl**

Abstract Light-induced reaction dynamics of isolated photosynthetic membranes obtained from wild-type (WT) and reaction center (RC)-subunit deletion strains SPUHK1 (an H-subunit deletion mutant) and SKΔLM (an (L+M) deletion mutant) of the purple non-sulphur bacterium *Rhodospirillum rubrum* have been investigated by femtosecond transient absorption spectroscopy. Upon excitation of the spirilloxanthin (Spx) S_2 state at 546 nm, of the bacteriochlorophyll Soret band at 388 nm and probing spectral regions, which are characteristic for carotenoids, similar dynamics in the SPUHK1, SKΔLM and WT strains could be observed. The excitation of Spx S_2 is followed by the simultaneous population of the lower singlet excited states S_1 and S^* which decay with lifetimes of 1.4 and 5 ps, respectively for the mutants, and 1.4 and 4 ps, respectively, for the wild-type. The excitation of the BChl Soret band is followed by relaxation into BChl lower excited states which compete with excitation energy transfer BChl-to-Spx. The deexcitation pathway BChl(Soret) $\rightarrow$ Spx(S_2) $\rightarrow$ Spx(S_1) occurs with the same transition rate for all investigated samples (WT, SPUHK1 and SKΔLM). The kinetic traces measured for the Spx $S_1 \rightarrow S_N$ transition display similar behaviour for all samples showing a positive signal which increases within the first 400 fs (i.e. the time needed for the excitation energy to reach the Spx S_1 excited state) and decays with a lifetime of about 1.5 ps. This suggests that the Spx excited state dynamics in the investigated complexes do not differ significantly. Moreover, a longer excited state lifetime of BChl for SPUHK1 in comparison to WT was observed, consistent with a photochemical quenching channel present in the presence of RC. For long delay times, photobleaching of the RC special pair and an electrochromic blue shift of the monomeric BChl *a* can be observed only for the WT but not for the mutants. The close similarity of the excited state decay processes of all strains indicates that the pigment geometry of the LH1 complex in native membranes is unaffected by the presence of an RC and allows us to draw a model representation of the WT, SKΔLM and SPUHK1 PSU complexes.

Abbreviations

LH1	Light-harvesting complex 1
RC	Reaction center
BChl	Bacteriochlorophyll
Spx	Spirilloxanthin
PSU	Photosynthetic unit
NIR	Near-infrared
ESA	Excited state absorption
TA	Transient absorption
EET	Excitation energy transfer
cryoem	Cryoelectron microscopy
AFM	Atomic force microscopy
SM	Single molecule

S. Amarie · M. O. Lenz · J. Wachtveitl (✉)
Institute for Physical and Theoretical Chemistry, Institute of Biophysics, Johann Wolfgang Goethe-University Frankfurt, Max-von-Laue-Str. 7, Building N120/224, 60438 Frankfurt am Main, Germany
e-mail: wveitl@theochem.uni-frankfurt.de

D. Lupo · R. Saegesser · R. Ghosh
Department of Bioenergetics, Institute of Biology, University of Stuttgart, Pfaffenwaldring 57, 70550 Stuttgart, Germany

Introduction

It is well-established (see Law et al. 2004), that the carotenoids of purple bacteria are exclusively bound to the protein components of the photosynthetic unit (PSU), which consists of a reaction center (RC) surrounded by a light-harvesting complex (LH1). For many purple bacteria including the one employed in this study *Rhodospirillum rubrum*, the RC is a heterotrimer, containing the membrane-bound subunits, L and M, which bind the bacteriochlorophyll (BChl) "special pair", two accessory BChls, two bacteriopheophytins (BPh), two quinone molecules, as well as one molecule of carotenoid (spirilloxanthin (Spx)) (see Law et al. 2004; Koyama et al. 2008). The LM dimer associates strongly with the RC-H-subunit, which consists of a single transmembrane helix attached to a large cytoplasmically located polar domain adhering to the cytoplasmically exposed surface of the LM dimer. For *R. rubrum*, medium-resolution images of 2D crystals of the PSU have suggested that the RC is completely enclosed by the LH1 complex, which consists of a ring-like array of 16 subunits formed from the non-identical α and β polypeptides (Karrasch et al. 1995; Jamieson et al. 2002). Biochemical evidence has indicated that each αβ subunit binds a pair of BChls and one Spx molecule (Picorel and Gingras 1983; Cogdell et al. 1982). So far, the low resolution of the images obtained by cryo-electron microscopy (cryo-EM) (Jamieson et al. 2002; Karrasch et al. 1995) does not allow the assignment of the 16 Spx molecules to the inner or outer surface of the LH1 ring. Both the cryo-EM data (Jamieson et al. 2002; Karrasch et al. 1995) as well as current models (Fotiadis et al. 2004; Schulten 1999) of the PSU place the RC against the wall of the LH1 ring, without necessitating its structural distortion. However, the structural interaction of the *R. rubrum* LH1 complex with the RC is subject to some controversy. On the one hand, results obtained by atomic force microscopy (AFM) (Fotiadis et al. 2004; Scheuring et al. 2004) and low-resolution cryo-EM (Jamieson et al. 2002) from 2D-crystals of the RC-LH1 PSU indicate significant ellipticity of the LH1 ring, consistent with a single molecule (SM) spectroscopic study (Ketelaars et al. 2002) of detergent-solubilized PSUs. However, the geometrical interpretation of the AFM studies may be biased due to packing forces, since in the study of Fotiadis et al. (Fotiadis et al. 2004), removal of the H-subunit did not affect the ellipticity of the *R. rubrum* LH1, whereas in the AFM study of Scheuring et al. (Scheuring et al. 2004) performed on intact photosynthetic membranes of *Rhodobacter blasticus*, removal of the H-subunit appeared to cause the LH1 complex to become circular. A complication here, in addition to the low resolution of the data, is that the *R. blasticus* PSU appears to be an RC-LH1 dimer, also containing the PufX polypeptide,

which has been implicated in quinone transfer across the LH1 ring (Farchaus et al. 1993; Wachtveitl et al. 1993), whereas the *R. rubrum* PSU, which lacks PufX (Bèlanger et al. 1988), appears to be a closed unit. On the other hand, SM spectroscopic studies performed on PSUs isolated by the Ghosh group have indicated no perturbation of the LH1 circular symmetry due to the presence of an RC (Gerken et al. 2003) either when solubilized in detergent or reconstituted into bilayer membranes. Nevertheless, both the low resolution (4 Å) crystal structure (Roszak et al. 2003) and SM spectroscopy (Richter et al. 2007) of a detergent-solubilized PSU from *Rhodopseudomonas palustris*, as well as AFM images of the PSU in intact membranes of *Rhodospirillum photometricum* (Scheuring et al. 2004) also indicate an elliptical geometry of the LH1 ring.

It appeared to us that if a significant distortion from LH1 circular symmetry is present, this might affect the relative distances between the BChl and Spx molecules, thus perhaps affecting also the rates of energy transfer between them (Blankenship 2002; van Amerongen et al. 2000). This expectation is complicated by a number of considerations: (i) the precise mechanism of energy transfer between BChls and Spx is controversial, but it now seems likely that either a Dexter exchange mechanism or Coulombic interaction, and not Förster energy transfer are probably operative; (ii) the positions of the carotenoids within the LH1 structure are not known. However, both of these objections do not necessarily obviate our expectations. In particular, it has been conclusively shown by Raman spectroscopy (Kuki et al. 1995) that the Spx is in the *all-trans* conformation and spans the membrane in close association with the LH1 polypeptides (as evidenced by the maintenance of the BChl/Spx stoichiometry, even in detergent-solubilized PSUs). In addition, since the assembly and expression of the LH1 is not dependent on the presence of carotenoid (in contrast to the assembly of LH2 complexes, where the carotenoids are arranged between the polypeptide chains (McDermott et al. 1995) and contribute decisively to the stability of the complex (McDermott et al. 1995)), as well as the fact that 2D crystals of Spx-containing LH1 complexes crystallize with a completely different space group to those of carotenoid-less LH1 complexes, it seems highly likely that the Spx molecules are arranged on the outer surface of the LH1 ring. Preliminary molecular modelling of the LH1 complexes (R. Ghosh, unpublished) shows that any structurally reasonable (the distances must still be sufficient to account for Spx-BChl energy transfer) positioning of the Spx molecules at the αβ(BChl)₂ interface would place them no more than a few angstroms from the αβ-BChl pair. Since both the Dexter and Coulombic exchange mechanisms are highly distance-dependent (much more so than the Förster mechanism), it seems likely that geometrical distortion of the LH1 complex

would affect energy transfer. Since all PSUs are affected equally, even an ensemble measurement might highlight these differences. This consideration provided a major motivation to compare the ultrafast pathways of BChl-Spx energy transfer in chromatophores obtained from WT *R. rubrum* to those of mutants lacking either the complete RC (mutant SPUHK1 (Lupo and Ghosh 2004)) or the L and M subunits (mutant SKΔLM (Saegesser 1994)).

The WT carotenoid of *R. rubrum*, spirilloxanthin contains 13 conjugated double bonds and is so far the most unsaturated carotenoid known to be involved in photosynthetic light harvesting. It is well-accepted (Gradinaru et al. 2001; Okamoto et al. 1998; Polivka and Sundström 2009; Hashimoto et al. 2004; Polivka and Sundström 2004) that the three major absorption maxima (at 485, 520, and 546 nm) of Spx correspond to vibronic levels of the second excited S_2 state, with the first excited states S_1 (also designated the $2A_g^-$ state) and S* (see below) being symmetry-forbidden for the initial excitation process. Immediately following excitation, the S_2 state rapidly decays within 60–200 fs (Gradinaru et al. 2001) to the S_1 and S* state. From the S_1 state, the system either decays to the ground state or energy transfer to the Q_y state of BChl can potentially occur (Gradinaru et al. 2001). However, as a consequence of its extended conjugation, the S_1 state of Spx is short-lived and decays to the ground state in 1.4 ps both in solution and when bound to the LH1 complex of *R. rubrum* S1 (WT strain) in native membranes (Gradinaru et al. 2001). In isolated LH1 complexes, a slightly longer decay time of 1.6–1.7 ps has been observed (Okamoto et al. 1998). This indicates that no energy transfer can occur from the Spx S_1 state to the Q_y state of BChl, resulting in the low total efficiency of Spx to BChl energy transfer of 30% (Gradinaru et al. 2001).

The availability of two independent RC-less mutant strains, both of which exhibit spectroscopic properties characteristic of intact LH1 complexes (see below), allows us to define the excitation energy transfer (EET) pathways between LH1 pigments more precisely than previously possible.

Materials and methods

Sample preparation

Chromatophore membranes were obtained from either the wild-type (S1) or the S1-derived deletion mutants SPUHK1 (containing a lesion in the *puhA* gene (Lupo and Ghosh 2004)) or SKΔLM (which lacks both L and M subunits (Saegesser 1994)). In the SKΔLM a Tn908-derived kanamycin cassette was substituted for the BstEI-SalI fragment (which flanks both the L and M subunits) of the chromosomal *puf* operon (Bèlanger et al. 1988) using site-directed

mutagenesis. This strain completely lacks L and M subunits but retains the H-subunit, which localizes to the PSU (R. Ghosh, unpublished data). To facilitate a meaningful comparison, all strains were grown semi-aerobically using the medium M2SF, which induces photosynthetic membrane levels normally obtained only under low light conditions in the absence of oxygen (Ghosh et al. 1994).

Chromatophores were prepared as described (Lupo and Ghosh 2004) and diluted in 20 mM Tris-HCl (pH 8.0) containing 10 mM sodium ascorbate. The typical sample OD was 0.3–0.6/mm at 520 nm. Sample stability was confirmed by measuring the absorption spectra before and after the time-resolved measurements. Fused silica cuvettes with a pathlength of 1 mm were used for measurements. Determination of the BChl content of the wild-type and SPUHK1 chromatophores yielded a values of 33 ± 4 nmol of BChl/mg protein (Lupo and Ghosh 2004) and 33 ± 2 nmol BChl/mg protein, respectively. These values are almost identical to that (34 ± 5 nmol of BChl/mg protein) reported by Cheng et al. (Cheng et al. 2000) for chromatophores from photoheterotrophically grown cells.

To minimize accumulation of photoproduct, the sample was translated continuously both horizontally and vertically in a direction normal to the bisector of the pump and probe beams at ∼10 cm/s.

Stationary and time-resolved spectroscopy measurements

Absorption spectra were recorded with an Analytik Jena (Jena, Germany) S100 spectrometer using 1 mm fused silica cuvettes. The time-resolved measurements using the femtosecond pump/probe technique were performed with a setup based on a CLARK CPA 2001 (Dexter, MI) laser/amplifier system operating at a repetition rate of ∼1 kHz and at a central wavelength of 775 nm. The pulse width of the system was around 150 fs (FWHM). The laser served as pulse source for the following nonlinear processes. Excitation pulses were generated using a non-collinear optical parametric amplifier (NOPA) (Huber et al. 2001; Wilhelm et al. 1997) and by second harmonic generation (SHG). For carotenoid excitation, laser pulses of 50 fs duration and 15 nm spectral bandwidth at a central wavelength of 546 nm were used. While for BChl excitation, the laser pulse characteristics were: 150 fs duration, 5 nm bandwidth and 388 nm central wavelength. The pulses were focused to a diameter of about 100 μm inside the cuvette. The pulse energies were around 15 nJ for the 546 nm excitation and 45 nJ for the 388 nm excitation, small enough to prevent multi-photon excitation of the sample. The sample was probed with a white light continuum generated by focusing the 775 nm beam onto a 2 mm thick sapphire plate, whereby a spectral range of

400–1000 nm was used for probing. The continuum pulses were dispersed by two VIS-spectrometers, (sample and reference) and recorded with two 42 segment diode arrays. Data acquisition was performed in single shot detection mode as balanced and referenced measurement providing signal to noise ratios up to 10^{-4} (Amarie et al. 2007). Excitation and probe pulses were polarized parallel. To account for long term drifts and possible degradation of the sample, the ratio between probe and reference signals for the non-excited sample was determined for every third shot.

Results

Steady-state absorption spectroscopy

Figure 1a shows the absorption spectra of wild-type (S1) and the H (SPUHK1) and L+M (SKΔLM) deletion mutants. All complexes show the characteristic three-peak structure of Spx with a Franck–Condon (0–0) transition at 550 nm. In addition, antenna BChls contribute to the spectrum with three main bands, namely the Soret band (375 nm), the Q_x (590 nm) and Q_y absorption bands (882 nm), respectively. The WT spectrum also shows two smaller additional peaks at 760 and 802 nm attributable to the Q_y transitions of the RC-bound BPh and accessory BChl, respectively (Farchaus et al. 1993; Wachtveitl et al. 1993). The absorption maximum of the special pair, which normally contributes about 5% of the PSU absorption at 875 nm (Farchaus et al. 1993; Wachtveitl et al. 1993) is hidden underneath the Q_y band of the LH1 complex. With the exception of a small (~2 nm) red shift of the LH1 band compared to the WT, the absorption spectra bands of both mutants are identical in form and relative amplitude.

Excited state dynamics of wild-type, SPUHK1 and SKΔLM mutants of *R. rubrum* PSU following excitation of the spirilloxanthin S_2 state

To investigate the excited state dynamics of carotenoids and BChls in the photosynthetic unit complex of *R. rubrum* for WT, SKΔLM and SPUHK1, we performed time-resolved transient absorption (TA) experiments exciting the LH1 carotenoids to their S_2 excited state with a 546 nm laser pulse. Kinetic traces were measured over a broad spectral range for both visible as well as near-IR regions at a probing window from 400 to 1100 nm.

The excited state processes which occur upon carotenoid excitation in a LH1 are summarized in Fig. 2. A depopulation of the carotenoid ground state occurs upon excitation, which causes a negative (bleach) signal in the difference transient absorption spectrum around 500 nm; a
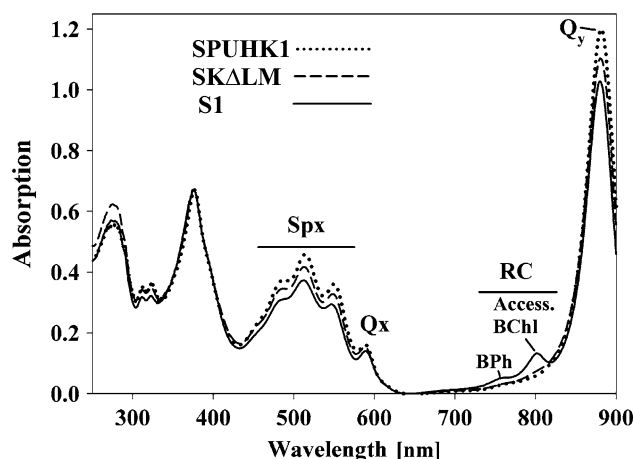

Fig. 1 Absorption spectrum of the chromatophore membranes from the WT (*solid line*) SPUHK1 and SKΔLM mutants. The peaks at 760 and 802 nm correspond to BPh and the RC-accessory BChl (absent in the SPUHK1 and SKΔLM). The spectra have been slightly offset for clarity. The absence of the RC polypeptides was also confirmed by SDS–PAGE (data not shown)

mirror image of the $S_0 \rightarrow S_2$ absorption band. Due to its direct excitation, an excited state absorption (ESA) band from S_2 arises in the spectral region above 950 nm (the $S_2 \rightarrow S_N$ transition) and least for a few hundred of femtoseconds. The S_2 excited state is depopulated in about 0.2 ps through different processes: an internal conversion (IC) into intermediate lower excited states, which results in a transient population of the S_1 excited state, visible as an ESA ($S_1 \rightarrow S_N$ transition) with a maximum at 620 nm, together with a population of the S* excited state leading also to a characteristic ESA around 600 nm. In parallel, excitation energy transfer to LH1 BChls can successfully compete with $S_2 \rightarrow S_1/S_2 \rightarrow$ S* IC, which will lead to a bleaching of the BChl band (880 nm) and concomitant an BChl ESA signal will arise around 840 nm.

At this point, we will concentrate our analysis on the excited state dynamics of S_1 excited state and on the excitation energy transfer Spx-to-BChl, since both are sensitive to the local environment of the Spx molecule. Accordingly, if the distances or the relative position between the BChl and Spx molecules is changed among WT, SKDLM and SPUHK1, due to the distortion from LH1 circular symmetry, it should affect the rates of energy transfer Spx-to-BChl and the excited state dynamics of Spx.

TA spectra recorded in the visible region (400–700 nm) were analysed by a global fitting routine and four decay components were sufficient to obtain an excellent global fit (Fig. 3). For both WT and SPUHK1, the fastest component (less than 200 fs) shows a negative amplitude between 500 and 620 nm and a positive signal with a maximum at 650 nm. The fast decay time allows us to assign this

Fig. 2 Schematic representation of energy levels and energy-transfer pathways between Spx and BChl *a* in the LH1 complex (*left*). Transient absorption data of WT LH1, upon carotenoid excitation at 546 nm (*right*). The S$_1$ level has been assigned to a value obtained from solution spectra of the isolated Spx
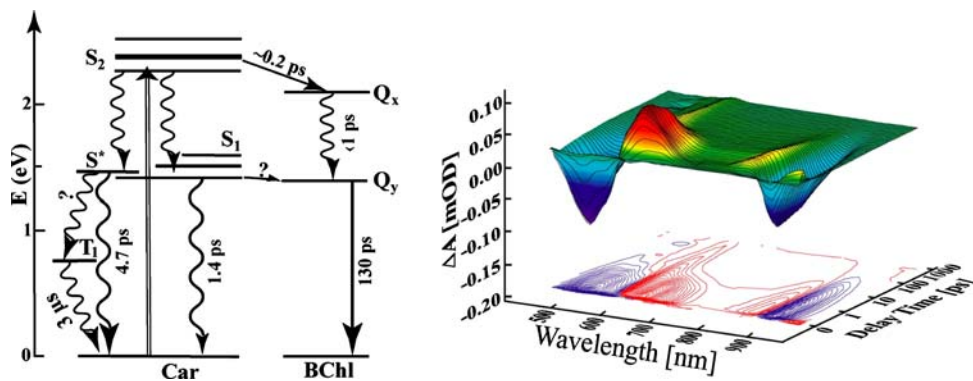
component to the decay of the S$_2$ state. The second component (Fig. 3, short dashed line) exhibits a time constant of approximately 1.4 ps and shows the characteristic spectral signature of the S$_1$ state (Gradinaru et al. 2001; Okamoto et al. 1998), with an excited state absorption (ESA) at 620 nm as well as a ground state bleaching with a negative minimum at about 510 nm. The amplitude associated with the time constant of 1.4 ps of the WT ESA is slightly smaller than that of SPUHK1. The global fit yields values for the third time constant of 3.8 ps for the WT and 4.7 ps for the SPUHK1 sample. The WT sample shows a larger overall amplitude and for both samples the loss of bleach is accentuated, and the ESA contribution dominates the spectra for λ_{probe} above 550 nm. The amplitude is negligible for wavelengths longer than 650 nm, and a small shoulder appears at 535 nm. Both the shape of the spectrum and the lifetime of this state are similar to those reported for the excited Spx S* state (Gradinaru et al. 2001). The last component represents a long-lived species not decaying on the time-scale of our experiment (1.5 ns). For both samples, this last component shows a weak negative contribution around 500 nm, a positive signal with a maximum centred at 575 nm and a smaller shoulder at 535 nm. We interpret this component as corresponding to the Spx triplet state. All of the above-mentioned spectral components can also be observed for the LM-deletion mutant SKΔLM (Fig. 3c). Taken together with the results for SPUHK1, this indicates that the spectral evolution of LH1 Spx after S$_2$ excitation is not affected by the presence of any RC components.

Near-IR transients contain mostly information on energy transfer within LH1 and from the carotenoid S$_2$ excited state to the LH1 BChls. Figure 4 shows TA spectra for WT LH1 at five different time delays after photoexcitation at 546 nm. After the pump pulse, the prompt appearance of a broad photoinduced ESA band, above 950 nm is observed (PA$_2$). Concomitant an ESA band termed PA$_1$ originally appearing at 750 nm shifts its maximum towards higher energies within 300 fs, displaying other kinetics than PA$_2$, indicating different origin. The PA$_2$ band decays very

quickly and is replaced, within ∼200 fs, by another ESA band peaking at 830 nm and a negative signal around 880 nm, the PA$_B$ and PB$_B$ bands. The PA$_1$ band is a well-known feature of carotenoids (Cerullo et al. 2001; Shreve et al. 1991), and is assigned to the S$_1 \rightarrow$ S$_N$ absorption, thus providing a spectral signature of the internal conversion process S$_2$-to-S$_1$. The PA$_2$ band was also previously observed (Yoshizawa et al. 2001; Zhang et al. 2001) and attributed to transient absorption from the S$_2$ state (S$_2 \rightarrow$ S$_N$ transition). Furthermore, we assigned PA$_B$ and PB$_B$ to transient absorption of BChl and bleach of the Q$_y$ band according to (Novoderezhkin 1999; Novoderezhkin and Razjivin 1993), respectively. The very rapid decay of PA$_2$ and the corresponding rise of PA$_1$ and PA$_B$ highlight the initial S$_2$-to-S$_1$ internal conversion process and the excitation energy transfer towards the BChls. The slight delay of PA$_B$ compared to PB$_B$ indicates the internal conversion of BChl from Q$_x$ to Q$_y$ (Fig. 4).

A selection of characteristic transients showing the temporal response of the absorbance change of WT and SPUHK1 upon excitation at 546 nm are presented in Fig. 5. The solid curves are fits resulting from the global fit analysis. The kinetic traces at 800 nm (Fig. 5a) show solely the temporal evolution of the BChl ESA band for the SPUHK1 sample (red curve), displaying the exponentially decay of this ESA. On the other hand, the WT sample show a faster decay of the BChl excited state and an additional offset for times longer than 100 ps. The kinetics measured at 864 nm (Fig. 5b) represents the evolution of the BChl ESA for WT and SPUHK1 following Spx excitation at 546 nm. For both the samples, we observe a rapid absorption decrease which vanishes within the first few hundred femtoseconds followed by an absorption increase showing different kinetics for the investigated samples. The fast negative signal, which is similar for both samples, reflects the transition of the excitation energy into the lowest BChl excited state. For SPUHK1, the positive signal corresponds exclusively to the excited state kinetics of antenna BChl, while for the WT sample, the additional negative signal at longer delay times reflects the excitation
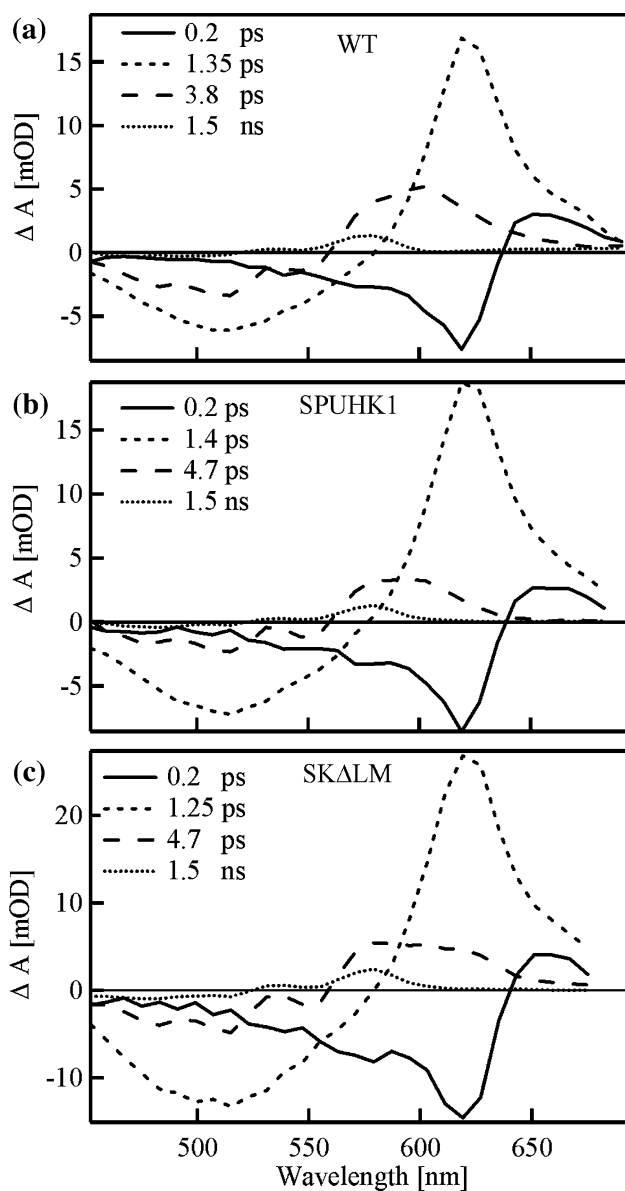
Fig. 3 Amplitude spectra (decay associated spectra) of the multiexponential global fit analysis for: **a** WT, **b** SPUHK1 and **c** SKΔLM mutant strains for the spectra obtained after excitation at 546 nm. The decay times for each component are indicated. Only the amplitudes for the WT and SPUHK1 strains have been normalized for the laser excitation intensity, and are therefore strictly comparable. The SKΔLM data, which was obtained in a separate experiment, is shown for the purposes of comparison of the spectral form and the corresponding decay times
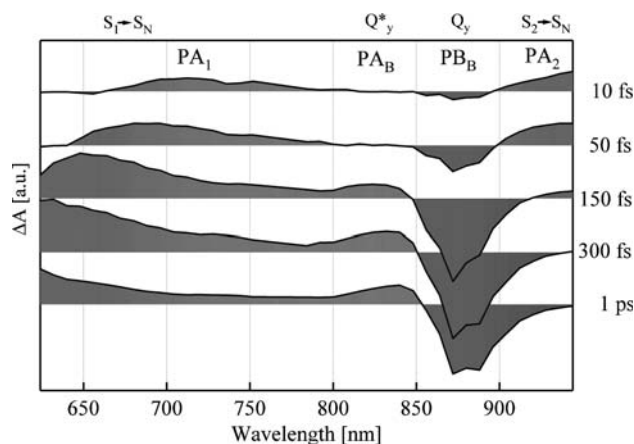

Fig. 4 Transient absorption spectra for WT sample at different time delays after photoexcitation at 546 nm

states to the BChl $Q_{x/y}$ states, since the 546 nm excitation pulse does not directly excite the BChls. The bleach signal grows within the first few hundred femtoseconds, i.e. the time needed for the excitation energy to reach the BChl. Note the same transfer rate, Spx to BChl, for both samples. The TA kinetics is followed by a significant loss of signal on the time scale of tens to hundreds of picoseconds. The observed loss is exclusively due to BChl dynamics which is spectrally separated from Spx. Clearly, SPUHK1 shows a longer lifetime of the excited state compared to WT, due to the lack of photochemical quenching pathways, i.e. excitation energy transfer to the RC. Last, the kinetic trace at 940 nm shows, additionally to the pattern presented for the 888 nm kinetic traces, a fast rise and decay of the PA_2, which is similar for both samples.

A global fit routine was applied to the data obtained in the near-IR spectral range (600–1100 nm) and revealed the presence of four components for WT and SPUHK1 mutant. Both samples have the first two components of <200 fs and 1.4 ps in common, which correspond to the time constants characteristic for excitation energy transfer towards BChls and Spx S_1 excited state dynamics. The third component of WT (46 ps) and SPUHK1 (130 ps) are mainly contributions of the excited BChl and the WT sample decays 3 times faster than the SPUHK1 sample, which can be attributed to excitation energy transfer to the RC, i.e. photochemical quenching. Other processes occurring in the LH1-RC complexes such as equilibration among BChls, and vibrational relaxation of BChl cannot be the main cause for these signals, as they occur on faster time scales and would manifest themselves as spectral changes (distribution of energy) whereas we observe an overall loss of electronic excitation. The slower processes are mainly associated with excited state decay via quenching channels (Monger and Parson 1976; Valkunas et al. 1996; Visser et al. 1995). Singlet–singlet annihilation of excitation

transfer to the RC. The 888 nm kinetic traces (Fig. 5c) show a large absorption decrease and were selected at the minimum of the Q_y BChl band, reflecting characteristic contributions from the BChl bleach at 880 nm and BChl stimulated emission at 920 nm. The transients at these wavelengths are thus dominated by the LH1 BChl excitation dynamics. The onset of the BChl bleach signal appears exclusively due to the energy transfer from Spx S_2/hot S_1

Fig. 5 Kinetic traces of the *R. rubrum* WT (*circles*) and SPUHK1 (*triangles*) mutant strain measured at 800, 864, 888 and 940 nm upon excitation at 546 nm. *Solid lines* represent the best fits obtained from multiexponential global fitting procedure
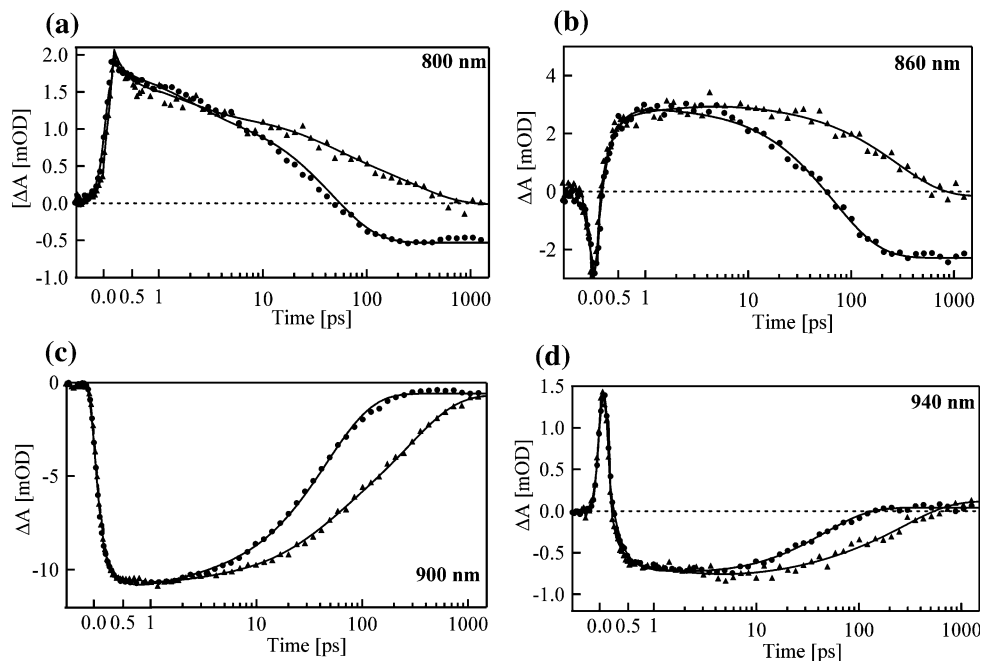
among and within LH1 rings can be also excluded because of the low excitation energy (van Grondelle 1985).

The last component describes a long time offset, i.e. the spectral amplitude at 1.5 ns. As seen in Fig. 6, the spectral amplitudes exhibit a well-defined shape for the WT, whereas for both mutants SKΔLM and SPUHK1 the defined structure is absent. At long delay times, almost all of the energy transfer and charge separation processes are expected to be completed. Therefore, the spectra reflect the differences in absorption between the charge-separated and the ground state. The main features in such a difference spectrum are caused by the photo-oxidation of the primary electron donor in the RC: i.e. bleach of the BChl dimer P band at around 880 nm. The electrochromic blue shift of the monomeric BChl *a* absorption band in the 800-nm region is reflected by an absorbance increase on the short-wavelength side of this band and a decrease at longer wavelengths. The loss of the interactions of the special pair of BChls with BChl *a* and the disappearance of the upper (i.e. higher energy) exciton transitions of the special pair may also add to the difference spectrum in this spectral range. No residual signal for long delay time was found for either of the mutants SPUHK1 or SKΔLM (Fig. 6), as expected from their RC-less phenotypes.

Excited state dynamics of wild type, SPUHK1 and SKΔLM mutants of *R. rubrum* PSU following excitation of the BChl soret band

To further strengthen our observations that the LH1 ring does not change its geometry upon removing a part or the
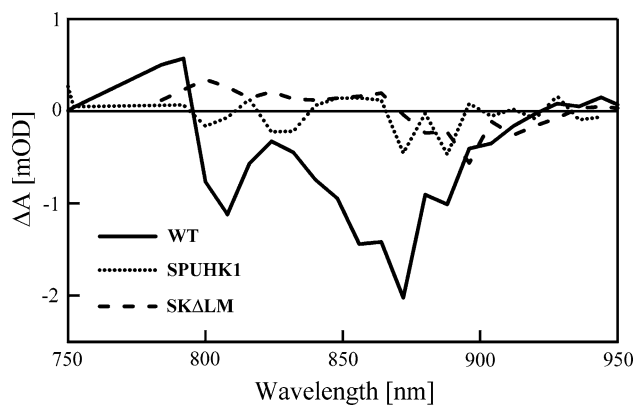

Fig. 6 Transient absorption difference spectra taken at 1.5 ns for WT (*solid line*), SPUHK1 (*dotted line*), and SKΔLM (*dashed line*) chromatophores of *R. rubrum*

complete RC, we now take a closer look at the excitation energy transfer BChl-to-Spx by performing TA measurements upon BChl Soret band excitation.

Figure 7 summarizes the excited state processes which occur within the first ps upon excitation of the BChl Soret band in a WT LH1. Initially, a depopulation of the BChl ground state occurs upon excitation, which causes a negative (bleach) signal in the difference transient absorption spectrum around 880 nm, and a BChl excited state absorption (ESA) band arises due to its direct excitation in the 800 nm spectral region. Furthermore, the S_2 excited state is populated as a consequence of the BChl-to-Spx EET which leads to the build up of an ESA above 940 nm ($S_2 \rightarrow S_N$ transition). The Spx S_2 excited state will then decay in about 0.2 ps through IC into intermediate lower

Fig. 7 Schematic representation of energy levels, energy-transfer and deexcitation pathways between BChl *a* and Spx in the LH1 complex (**a**) obtained from the transient absorption data (**b**) of WT LH1 upon BChl excitation at 388 nm
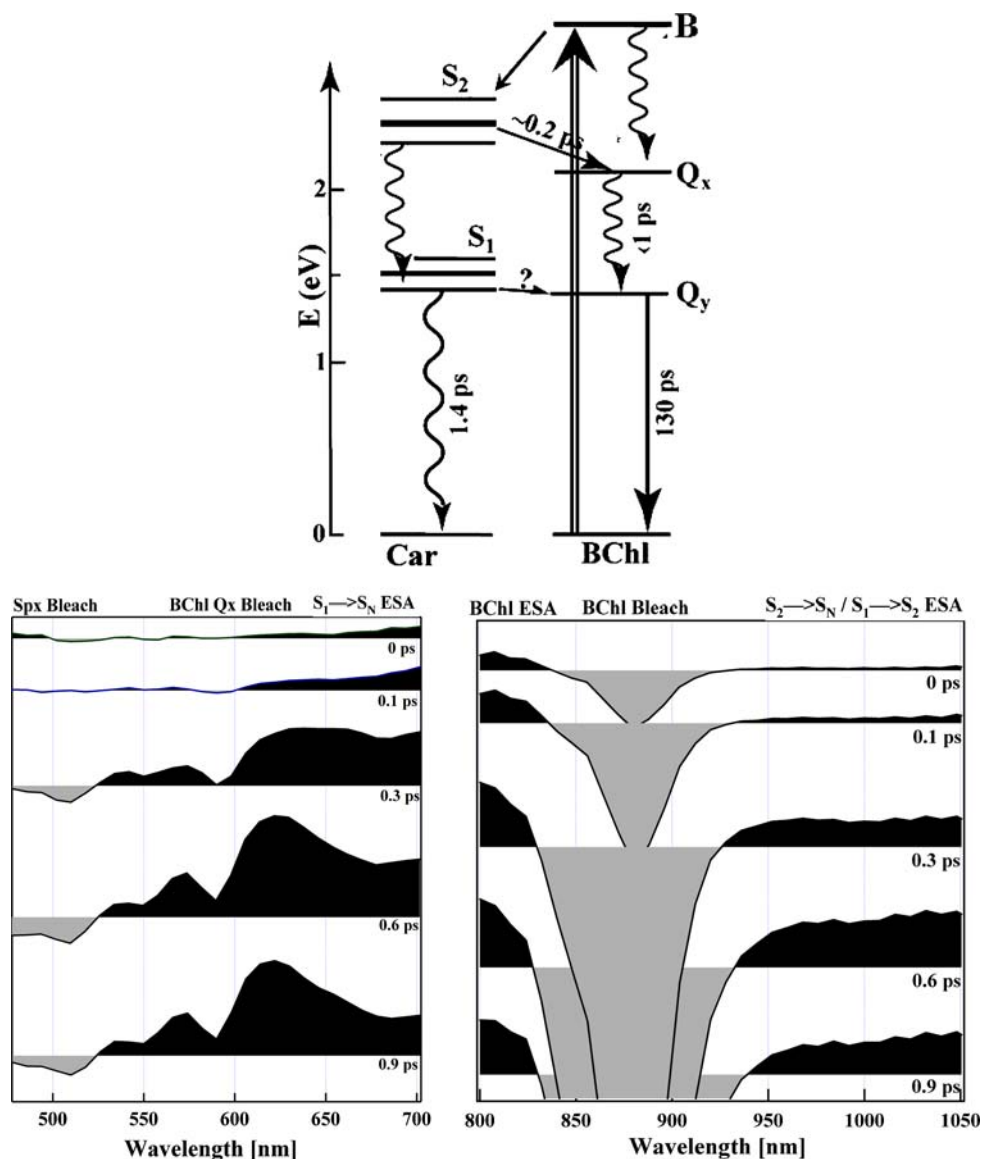
excited states, which results in a transient population of the S_1 excited state, visible as an ESA ($S_1 \rightarrow S_N$ transition) in the spectral region 600–700 nm.

Once again, if the distances or the relative position between the BChl and Spx molecules is changed among WT, SKΔLM and SPUHK1, due to the distortion from LH1 circular symmetry, it might also affect the rates of BChl-to-Spx energy transfer.

Figure 8 shows kinetic traces of WT, SKDLM and SPUHK1 recorded at 630 nm, i.e. the wavelength characteristic for the Spx $S_1 \rightarrow S_N$ transition. All investigated samples display, within the measurements errors, practically the same kinetics: a positive signal which increase within first 400 fs and decays with lifetimes of about 1.5 ps.
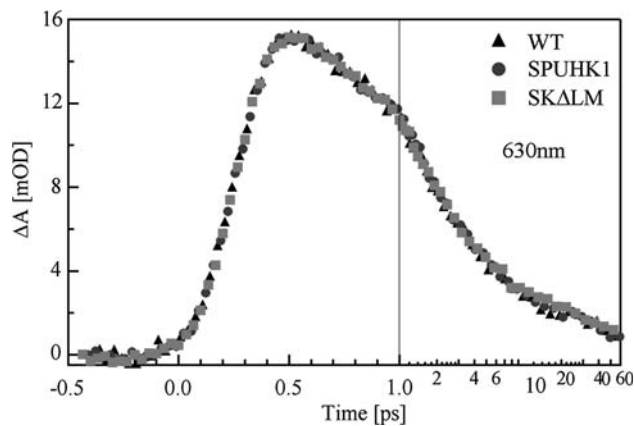

Fig. 8 Kinetic traces of the *R. rubrum* WT, SKΔLM and SPUHK1 mutant strains measured at 630 nm upon excitation at 388 nm

Discussion

The kinetics of excitation energy transfer between protein-bound pigments can be a very sensitive measure of the local environment. In this study, we have employed ultrafast spectroscopy to probe possible changes in the LH1-pigment organization in different mutants of *R. rubrum* lacking a functional RC, either due to the lack of the H-subunit, which is essential for RC-LM insertion into LH complexes, or due to site-directed deletion of the L and M subunits.

The decay kinetics of Spx for WT (S1) and the mutant samples following excitation at 546 nm show a very similar behaviour (Fig. 3). In particular, for both RC-less mutants, the excitation to the S_2 state is followed by the simultaneous population of the lower singlet excited states S_1 and S*, which then decay with lifetimes of approx. 1.4 and 4.7 ps, respectively, very close to the results found for WT (1.4 and 3.8 ps, respectively). The 4.7 ps lifetimes of S* in the mutants is similar to the ones found by Gradinaru et al. (Gradinaru et al. 2001) (5 ps) and Gärtner et al. (Gaertner et al. 2004) (3 ps), and is very close to the 3.8 ps found for the WT sample, suggesting that its dynamic properties in those complexes do not differ significantly.

Moreover, the deexcitation pathway BChl(Soret) $\rightarrow$ Spx(S_2) $\rightarrow$ Spx(S_1) occurs with the same transition rate for all investigated samples (WT, SPUHK1 and SKΔLM). This can be visualized by probing the $S_1 \rightarrow S_N$ transition of Spx upon BChl excitation into the Soret band (Fig. 8). The kinetic traces of all samples display similar behaviour showing a positive signal which increase within first 400 fs (i.e. the time needed for the excitation energy to reach the Spx S_1 excited state) and which decays with a lifetime of about 1.5 ps. The rise time of the ESA signal in Fig. 8 refers to the population of Spx S_1 excited state from the pumped BChl Soret band through Sxp $S_2 \rightarrow S_1$ internal conversion. Moreover, we have shown here that the $S_2 \rightarrow S_1$ relaxation is similar for all investigated samples. Hence, we can conclude that the EET from BChl to Spx occurs with the same time constant independent of RC mutation.

We have also shown for both SPUHK1 (Lupo and Ghosh 2004) and for the SKΔLM (R. Ghosh, unpublished data) that the near-IR CD spectra (which are a very sensitive measure of pigment–pigment interaction) are also identical to that of WT LH1. As stated in the introduction, a significant distortion from LH1 circular symmetry might affect the relative distances between the BChl and Spx molecules and might thus also alter the rates of energy transfer between them. Thus, by these criteria, the LH1 complex appears to be unperturbed by the presence of an RC. Based on these findings, we can draw now a model representation of the PSU complexes with the WT PSU as

being an LH1+RC complex, the SKΔLM PSU as containing the H-subunit but which lacks the pigment binding subunits L and M and the SPUHK1 PSU as a LH1 complex without the excitation energy acceptor RC (Fig. 9). However, we emphasize, that in view of the structural uncertainties of the LH1 model, in particular, the position of the Spx molecules with relation to BChl, our negative result does not yet provide an unambiguous proof that no distortion from circular symmetry is present in some or all of these complexes.

Employing femtosecond spectroscopy, we were able to track not only Spx excited states (S_2, S_1 and S*) and to monitor the excitation energy transfer from Spx-to-BChl or from BChl-to-Spx within the LH1 antenna, but also the energy transfer from LH1 to RC. The time-resolved difference absorption data at 800 and 864 nm (Fig. 5a and b) in a region where mostly ESA due to BChl is present, show a significantly different temporal behaviour of SPUHK1 and WT. The ESA grows instantaneously within 100 fs followed by a significant loss of signal on the time scale of tens to hundred of picoseconds. The observed loss derives exclusively from BChl dynamics which is separated from Spx. For SPUHK1, the BChl ESA signal (Fig. 5b) decays with the same time constant as the BChl bleach/SE (Fig. 5c) denoting that this ESA stems from the lowest BChl excited state, which relaxes directly into the ground state. The longer lifetime of the excited state for SPUHK1 in comparison to WT can be explained by the absence of the photochemical quenching channel. However, the BChl excited state lifetime for the SPUHK1 sample is much shorter than that of free BChl and also shorter than the lifetime observed in LH1 of other bacterial organisms. One possible explanation could be that the LH1 excited state lifetime is quenched due to energy transfer from the Bchl Q_y to the carotenoid S_1, like in quenched LHC II (Ruban et al. 2007). For long delay times, a characteristic signal remains for the WT sample due to the electrochromic blue shift of the monomeric BChl *a* and photobleaching of the special pair P (Fig. 6).

In summary, this study has allowed us to follow the complex dynamics of isolated photosynthetic membranes obtained from WT and different reaction center (RC)-subunit deletion strains. It could be shown that deletion of H or (L+M) subunits has no effect upon the Spx S_1, and only a very small effect upon the S* (from 4 ps WT to 5 ps SPUHK1) lifetimes of the overall LH1 complex. Moreover, the energy transfer from the excited Spx to the RC in the case of WT strain could be observed with a transfer time of about 46 ps. The absence of this deactivation channel for the RC-subunit deletion strains confirms the assignment of this essential quenching mechanism. Taken together, these results are consistent with the hypothesis derived from single molecule fluorescence data (Gerken et al. 2003) as
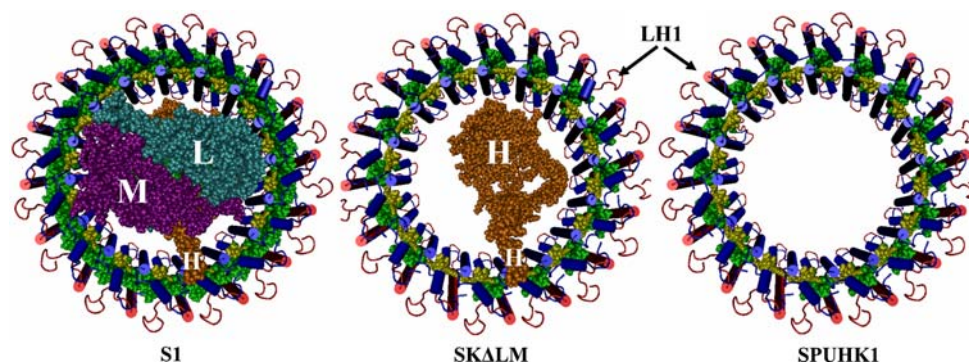
Fig. 9 Molecular models (R. Ghosh, F. Autenrieth, T. Ritz, and K. Schulten, unpublished data) of the intact PSU (LH1+RC) and the putative PSUs of SKΔLM (only the H-subunit of the RC is present) and, SPUHK1 as viewed from the periplasmic surface. The RC subunits L, M and H are indicated. In this model, the Spx has been arbitrarily assigned to the inner surface of the LH1 complex

well as from 2D crystals in vitro (Karrasch et al. 1995; Jamieson et al. 2002), that for the *R. rubrum* PSU, the presence of a RC has no effect upon the overall pigment organization of the LH1 complex in vivo.

References

Amarie S, Standfuss J, Barros T, Kuhlbrandt W, Dreuw A, Wachtveitl J (2007) Carotenoid radical cations as a probe for the molecular mechanism of nonphotochemical quenching in oxygenic photosynthesis. J Phys Chem B 111:3481–3487

Bèlanger G, Berard J, Corriveau P, Gingras G (1988) The structural genes-coding for the L-subunit and M-subunit of *Rhodospirillum rubrum* photoreaction center. J Biol Chem 263:7632–7638

Blankenship RE (2002) Molecular mechanisms of photosynthesis. Blackwell Science, Oxford/Malden

Cerullo G, Lanzani G, Zavelani-Rossi M, De Silvestri S (2001) Early events of energy relaxation in all-trans-beta-carotene following sub-10 fs optical-pulse excitation, Phys Rev B 63:241104(R)

Cheng YJS, Brantner CA, Tsapin A, Collins MLP (2000) Role of the H protein in assembly of the photochemical reaction center and intracytoplasmic membrane in *Rhodospirillum rubrum*. J Bacteriol 182:1200–1207

Cogdell RJ, Lindsay JG, Valentine J, Durant I (1982) A Further Characterization of the B890 Light-Harvesting Pigment Protein Complex from *Rhodospirillum rubrum* Strain-S1. FEBS Lett 150:151–154

Farchaus JW, Wachtveitl J, Mathis P, Oesterhelt D (1993) Tyrosine-162 of the photosynthetic reaction-center L-subunit plays a critical role in the cytochrome-C(2) mediated rereduction of the photooxidized bacteriochlorophyll dimer in *Rhodobacter sphaeroides*. 1. Site-directed mutagenesis and initial characterization. Biochemistry 32:10885–10893

Fotiadis D, Qian P, Philippsen A, Bullough PA, Engel A, Hunter CN (2004) Structural analysis of the reaction center light-harvesting complex I photosynthetic core complex of *Rhodospirillum rubrum* using atomic force microscopy. J Biol Chem 279:2063–2068

Gaertner P, Port H, Branschaedel M, Ghosh R (2004) FS-study on energy relaxation in light-harvesting (LH1) complexes from *Rhodospirillum rubrum* with carotenoids of different conjugation length. J Lumin 108:111–116

Gerken U, Lupo D, Tietz C, Wrachtrup J, Ghosh R (2003) Circular symmetry of the light-harvesting 1 complex from *Rhodospirillum rubrum* is not perturbed by interaction with the reaction center. Biochemistry 42:10354–10360

Ghosh R, Hardmeyer A, Thoenen I, Bachofen R (1994) Optimization of the sistrom culture-medium for large-scale batch cultivation of *Rhodospirillum rubrum* under semiaerobic conditions with maximal yield of photosynthetic membranes. Appl Environ Microbiol 60:1698–1700

Gradinaru CC, Kennis JTM, Papagiannakis E, van Stokkum IHM, Cogdell RJ, Fleming GR, Niederman RA, van Grondelle R (2001) An unusual pathway of excitation energy deactivation in carotenoids: singlet-to-triplet conversion on an ultrafast time-scale in a photosynthetic antenna. Proc Natl Acad Sci USA 98:2364–2369

Hashimoto H, Yanagi K, Yoshizawa M, Polli D, Cerullo G, Lanzani G, de Silvestri S, Gardiner AT, Cogdell RJ (2004) The very early events following photoexcitation of carotenoids. Arch Biochem Biophys 430:61–69

Huber R, Satzger H, Zinth W, Wachtveitl J (2001) Noncollinear optical parametric amplifiers with output parameters improved by the application of a white light continuum generated in CaF2. Opt Commun 194:443–448

Jamieson SJ, Wang PY, Qian P, Kirkland JY, Conroy MJ, Hunter CN, Bullough PA (2002) Projection structure of the photosynthetic reaction centre-antenna complex of *Rhodospirillum rubrum* at 8.5 angstrom resolution. EMBO J 21:3927–3935

Karrasch S, Bullough PA, Ghosh R (1995) The 8.5-angstrom projection map of the light-harvesting complex-I from *Rhodospirillum rubrum* reveals a ring composed of 16 subunits. EMBO J 14:631–638

Ketelaars M, Hofmann C, Kohler J, Howard TD, Cogdell RJ, Schmidt J, Aartsma TJ (2002) Spectroscopy on individual light-harvesting 1 complexes of *Rhodopseudomonas acidophila*. Biophys J 83:1701–1715

Koyama Y, Kakitani Y, Watanabe Y (2008) In: Renger G (ed) Primary processes of photosynthesis—part 1. Royal Society of Chemistry, Cambridge, UK, pp 151–201

Kuki M, Naruse M, Kakuno T, Koyama Y (1995) Resonance Raman evidence for 15-cis to all-trans photoisomerization of spirilloxanthin bound to a reduced form of the reaction center of *Rhodospirillum rubrum* S1. Photochem Photobiol 62:502–508

Law CJ, Roszak AW, Southall J, Gardiner AT, Isaacs NW, Cogdell RJ (2004) The structure and function of bacterial light-harvesting complexes (Review). Mol Membr Biol 21:183–191

Lupo D, Ghosh R (2004) The reaction center H subunit is not required for high levels of light-harvesting complex 1 in *Rhodospirillum rubrum* mutants. J Bacteriol 186:5585–5595

McDermott G, Prince SM, Freer AA, Hawthornthwaite-Lawless AM, Papiz MZ, Cogdell RJ, Isaacs NW (1995) Crystal structure of an integral membrane light-harvesting complex from photosynthetic bacteria. Nature 374:517-521

Monger TGCRJ, Parson W (1976) Triplet states of bacteriochlorophyll and carotenoids in chromatophores of photosynthetic bacteria. Biochim Biophys Acta 449:136–153

Novoderezhkin VaFZ (1999) Exciton delocalization in the B808–866 antenna of the green bacterium chloroflexus aurantiacus as revealed by ultrafast pump-probe spectroscopy. Biophys J 77:424–430

Novoderezhkin VI, Razjivin AP (1993) Excitonic interactions in the light-harvesting antenna of photosynthetic purple bacteria, their influence on picosecond absorbance difference spectra. FEBS Lett 330:5–7

Okamoto H, Ogura M, Nakabayashi T, Tasumi M (1998) Sub-picosecond excited-state dynamics of a carotenoid (spirilloxanthin) in the light-harvesting systems of *Chromatium vinosum*. Relaxation process from the optically allowed S-2 state. Chem Phys 236:309–318

Picorel RB, Gingras G (1983) Antenna holochrome B880 of *Rhodospirillum rubrum* S1. Pigment, phospholipid, and polypeptide composition. Biochemistry 22:2491–2497

Polivka T, Sundström V (2004) Ultrafast dynamics of carotenoid excited states. Chem Rev 104:2021–2072

Polivka T, Sundström V (2009) Dark excited states of carotenoids: consensus and controversy. Chem Phys Lett 477:1–11

Richter MF, Baier J, Southall J, Cogdell RJ, Oellerich S, Köhler J (2007) Refinement of the X-ray structure of the RC–LH1 core complex from *Rhodopseudomonas palustris* by single-molecule spectroscopy. Proc Natl Acad Sci 104:20280–20284

Roszak AW, Howard TD, Southall J, Gardiner AT, Law CJ, Isaacs NW, Cogdell RJ (2003) Crystal structure of the RC-LH1 core complex from *Rhodopseudomonas palustris*. Science 302:1969–1972

Ruban AV, Berera R, Ilioaia C, van Stokkum IHM, Kennis JTM, Pascal AA, van Amerongen H, Robert B, Horton P, van Grondelle R (2007) Identification of a mechanism of photoprotective energy dissipation in higher plants. Nature 450:575–578

Saegesser R (1994) Identifikation uns Charakterisierung des Photosynthese-Genclusters von *Rhodospirillum rubrum*. PhD thesis, University of Zurich, Zurich

Scheuring S, Francia F, Busselez J, Melandri BA, Rigaud JL, Levy D (2004a) Structural role of PufX in the dimerization of the photosynthetic core complex of *Rhodobacter sphaeroides*. J Biol Chem 279:3620–3626

Scheuring S, Sturgis JN, Prima V, Bernadac A, Levy D, Rigaud JL (2004b) Watching the photosynthetic apparatus in native membranes. Proc Natl Acad Sci USA 101:11293–11297

Schulten K (1999) Simplicity and complexity in proteins and nucleic acids, Vol. From simplicity and back, Dahlem University Press, Berlin

Shreve AP, Trautman JK, Owens TG, Albrecht AC (1991) Determination of the S2 lifetime of beta-carotene. Chem Phys Lett 178:89–96

Valkunas L, Akesson E, Pullerits T, Sundström V (1996) Energy migration in the light-harvesting antenna of the photosynthetic bacterium *Rhodospirillum rubrum* studied by time-resolved excitation annihilation at 77 K. Biophys J 70:2373–2379

van Amerongen H, Valkunas L, van Grondelle R (2000) Photosynthetic excitons. World Scientific, Singapore/River Edge

van Grondelle R (1985) Excitation-energy transfer, trapping and annihilation in photosynthetic systems. Biochim Biophys Acta 811:147–195

Visser HM, Somsen OJ, van Mourik F, Lin S, van Stokkum IH, van Grondelle R (1995) Direct observation of sub-picosecond equilibration of excitation energy in the light-harvesting antenna of *Rhodospirillum rubrum*. Biophys J 69:1083–1099

Wachtveitl J, Farchaus JW, Mathis P, Oesterhelt D (1993) Tyrosine-162 of the photosynthetic reaction-center L-subunit plays a critical role in the cytochrome-C(2) mediated rereduction of the photooxidized bacteriochlorophyll dimer in *Rhodobacter sphaeroides*. 2. Quantitative kinetic-analysis. Biochemistry 32:10894–10904

Wilhelm T, Piel J, Riedle E (1997) Sub-20-fs pulses tunable across the visible from a blue-pumped single-pass noncollinear parametric converter. Opt Lett 22:1494–1496

Yoshizawa M, Aoki H, Hashimoto H (2001) Vibrational relaxation of the $2A_g^-$ excited state in all-trans-beta-carotene obtained by femtosecond time-resolved Raman spectroscopy, Phys Rev B 63:180301(R)

Zhang JP, Skibsted LH, Fujii R, Koyama Y (2001) Transient absorption from the 1B(u)(+) state of all-trans-beta-carotene newly identified in the near-infrared region. Photochem Photobiol 73:219–222